

# New results on fully corrected dijet asymmetry in Pb+Pb collisions with ATLAS

Dennis V. Perepelitsa (on behalf of the ATLAS Collaboration)<sup>1</sup>

*Physics Department, Brookhaven National Laboratory, Upton NY, 11973 USA*

---

## Abstract

The phenomenon of events containing highly asymmetric dijet pairs is one of the most striking results in heavy ion physics, providing the first direct observation of in-medium jet energy loss at the Large Hadron Collider. Detailed measurements of a centrality-dependent dijet imbalance in 2.76 TeV Pb+Pb collisions using data collected by the ATLAS detector in the 2011 LHC heavy ion run are presented. The new analysis provides a measurement, fully corrected for detector effects to the particle level, of the centrality- and leading jet transverse momentum- ( $p_T$ -) dependence of the dijet  $p_T$  balance distribution, compared to an analogous measurement in  $pp$  collisions at the same center-of-mass energy.

**Keywords:** heavy ion physics, jet quenching, dijet asymmetry, energy loss

---

## 1. Introduction

Since the beginning of the heavy ion physics program at the Large Hadron Collider (LHC), measurements of the energy balance of dijets in lead–lead (Pb+Pb) collisions have been a valuable way to probe the differential energy loss of fast partons traversing the hot nuclear medium. Since the outgoing partons from a hard parton–parton scattering early in the collision generally traverse a different path length, they lose different amounts of energy. This phenomenon is typically quantified through the distribution of the dijet asymmetry values  $A_J \equiv (p_{T,1} - p_{T,2})/(p_{T,1} + p_{T,2})$  and dijet  $p_T$  balance ratio  $x_J \equiv p_{T,2}/p_{T,1}$ , where  $p_{T,1}$  and  $p_{T,2}$  indicate the transverse momentum of the leading and subleading jet in the event, respectively.

Initial measurements of  $A_J$  and  $x_J$  distributions in Pb+Pb collisions showed that they are modified in a centrality-dependent manner due to this path-length dependent energy loss [1], while remaining unmodified in  $p+Pb$  collisions [2]. Although these have generated much theoretical interest [3], the measured distributions have typically not been corrected for detector effects, making direct comparisons with jet quenching calculations ambiguous. Recent advances in jet measurement techniques in heavy ion collisions, including a quantitative determination of the heavy ion jet energy scale in ATLAS [4], have enabled more sophisticated measurements. This proceedings presents an updated measurement of the dijet  $p_T$  balance ratio in Pb+Pb and  $pp$  collisions [5] as a function of centrality and leading jet  $p_T$ , in which the distributions have been fully corrected to the particle level. Together with measurements of modified single and multi-jet production rates [6], these observables can provide a more complete picture of energy loss in the hot nuclear medium.

---

<sup>1</sup>A list of members of the ATLAS Collaboration and acknowledgements can be found at the end of this issue.

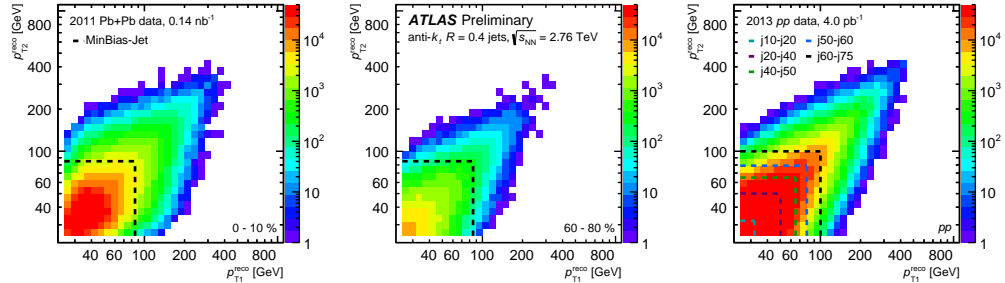


Fig. 1. Symmetrized distributions of the leading and subleading jet  $p_T$  in central (left) and peripheral (center) Pb+Pb collisions and in  $pp$  collisions (right), from Ref. [5]. The dashed lines indicate boundaries used in selecting different triggers.

## 2. Data selection and jet reconstruction

The data used in this work comprise  $0.14 \text{ nb}^{-1}$  of Pb+Pb data at  $\sqrt{s_{\text{NN}}} = 2.76 \text{ TeV}$  and  $4.0 \text{ pb}^{-1}$  of  $pp$  data at  $\sqrt{s} = 2.76 \text{ TeV}$  delivered by the LHC in 2011 and 2013, respectively. The ATLAS detector is described in detail in Ref. [7]. The hermetic, large-acceptance calorimeter system, which includes liquid argon (LAr) electromagnetic and hadronic calorimeters, and a steel-scintillator hadronic calorimeter, provided the jet energy measurement. The Pb+Pb data were selected using a combination of a minimum bias trigger, defined by a minimum amount of energy in the calorimeter system or a coincidence in the zero-degree calorimeters situated far downstream of the interaction point, and a hardware-based jet trigger. The centrality of Pb+Pb collisions is characterized using the sum of transverse energy in the forward calorimeter modules, situated at  $3.2 < |\eta| < 4.9^2$ . In  $pp$  collisions, the data were selected using high-level jet triggers with increasing  $p_T$  thresholds, in which the highest-threshold trigger sampled the full luminosity.

Jets were reconstructed according to a procedure that closely follows those used for previous measurements in Pb+Pb and  $pp$  collisions [8]. Calorimeter cells were collected into  $\Delta\eta \times \Delta\phi = 0.1 \times 0.1$  towers at the electromagnetic scale. An iterative procedure was used to determine the underlying event (UE) energy density in an  $\eta$ - and calorimeter layer-dependent manner, while excluding jets from that estimate. For this measurement, the UE estimation procedure was extended to allow for possible third- and fourth-order modulations of the energy density due to flow. Jets were defined by the application of the anti- $k_t$  algorithm with  $R = 0.4$  to the towers, with the kinematics of the jet updated to remove the UE contribution. The jet  $p_T$  was corrected for the response of the calorimeter with a calibration derived from simulation and for an additional, small data-to-simulation difference derived from *in situ* studies of the jet response [4].

## 3. Data analysis, corrections and systematics

Events selected for analysis were required to have the leading and sub-leading jet within  $|\eta| < 2.1$ , with  $p_{T,1} > 100 \text{ GeV}$  and  $p_{T,2} > 25 \text{ GeV}$ . Furthermore, the dijet configuration was required to be back-to-back as given by  $|\Delta\phi| > 7\pi/8$ . The triggered samples were weighted by their respective luminosity (in  $pp$  collisions) or corrected for their respective scaledowns (in Pb+Pb collisions) and used to populate the two-jet ( $p_{T,1}, p_{T,2}$ ) spectrum. Each  $p_{T,1}$  range was populated using only the highest-statistics trigger which was efficient in that range. The resulting distributions were symmetrized along the  $p_{T,1} = p_{T,2}$  axis to allow the unfolding to properly treat instances where the leading/subleading classification switched due to the fluctuations in the UE and response. Figure 1 shows representative two-jet distributions in Pb+Pb and  $pp$  collisions.

<sup>2</sup>ATLAS uses a right-handed coordinate system with its origin at the nominal interaction point (IP) in the centre of the detector and the  $z$ -axis along the beam pipe. The  $x$ -axis points from the IP to the centre of the LHC ring, and the  $y$ -axis points upward. Cylindrical coordinates  $(r, \phi)$  are used in the transverse plane,  $\phi$  being the azimuthal angle around the  $z$ -axis. The pseudorapidity is defined in terms of the polar angle  $\theta$  as  $\eta = -\ln \tan(\theta/2)$ .

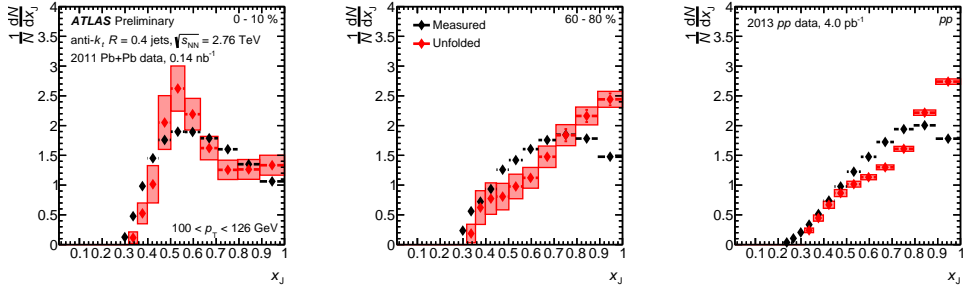


Fig. 2. Example of per-dijet  $x_J$  distributions at the detector-level (black) and after unfolding to the particle level (red), shown for  $p_{T,1} > 100$  GeV dijets in central (left) and peripheral (center) Pb+Pb collisions and in  $pp$  collisions (right), from Ref. [5].

Due to the presence of low- $p_T$  reconstructed jets which arise from UE fluctuations in Pb+Pb collisions, the  $(p_{T,1}, p_{T,2})$  distribution contains a residual contribution from the combinatoric pairing of leading jets with UE fluctuations. These pairings were found to occur when the UE fluctuations sit atop third- and fourth-order flow maxima, and the residual contribution was therefore modeled as  $C(\Delta\phi) = Y(1 + 2c_3 \cos 3\Delta\phi + 2c_4 \cos 4\Delta\phi)$ . For each  $(p_{T,1}, p_{T,2})$  interval, the values of  $c_3, c_4$  and  $Y$  were constrained in the region  $\Delta\phi < 1.4$  and used to estimate and subtract the combinatoric contribution in the signal region  $\Delta\phi > 7\pi/8$ . This contribution was 10% at the lowest  $x_J$  values in central collisions, and smaller elsewhere.

Monte Carlo simulations of hard scattering events, including a full GEANT4 simulation of the detector, were used to evaluate the performance of the dijet measurement [9]. PYTHIA was used to generate  $pp$  event samples [10], and a separate sample of PYTHIA events was overlaid onto Pb+Pb minimum bias data. To include possible correlations in the response of the leading and subleading jets, four-dimensional response matrices were generated between the particle-level and reconstructed jet pairs. A Bayesian unfolding procedure [11] was used to correct the bin migration in the measured  $(p_{T,1}, p_{T,2})$  distributions. The number of iterations was chosen by checking the stability against additional iterations and performing a refolding test.

For each  $p_{T,1}$  and centrality selection, the unfolded  $(p_{T,1}, p_{T,2})$  distributions were projected into  $x_J$  distributions. Figure 2 shows an example of  $x_J$  distributions before and after the unfolding procedure. Systematic uncertainties on the results were evaluated in the following ways: response matrices were generated with variations in the jet energy scale and resolution (most important at high- $p_T$  and in central collisions); the number of unfolding iterations was varied and the prior  $x_J$  distribution in simulation was reweighted (most important at low- $p_T$  and in peripheral collisions); the two-jet response was factorized into the product of the single jet response; and the procedure for determining the combinatoric dijet contribution was varied.

#### 4. Dijet asymmetry results

Figure 3 summarizes the corrected dijet  $p_T$  balance distributions. The left-most panels of Figure 3 show how the  $x_J$  distribution for  $100 < p_{T,1} < 126$  GeV dijets evolves with selections on event centrality. In the most peripheral Pb+Pb collisions, the  $x_J$  distributions are largest at unity and fall off at lower  $x_J$  values. They are consistent with the analogous distributions in  $pp$  collisions and indicate predominantly balanced dijet configurations. With increasingly more-central event selections, the  $x_J$  distribution shifts to lower values of  $x_J$ , indicating a higher prevalence of very asymmetric dijet configurations. In the most central events, the  $x_J$  distributions develop a peak near  $x_J \approx 0.5$ . Thus, in these events the most common dijet configuration after quenching is when the subleading jet has half the  $p_T$  of the leading jet.

The right-most panels of Figure 3 show how the  $x_J$  distribution in the most central collisions evolves with selections on the leading jet  $p_T$ . As shown above, for  $100 < p_{T,1} < 126$  GeV dijets, the  $x_J$  distribution in 0-10% Pb+Pb events is substantially different from that in  $pp$  collisions. However, for systematically higher  $p_{T,1}$  selections, the  $x_J$  distributions in Pb+Pb collisions shift to larger values of  $x_J$ . For  $p_{T,1} > 200$  GeV, the  $x_J$  distribution in central events is peaked at unity, and is qualitatively similar to that in  $pp$  collisions. This

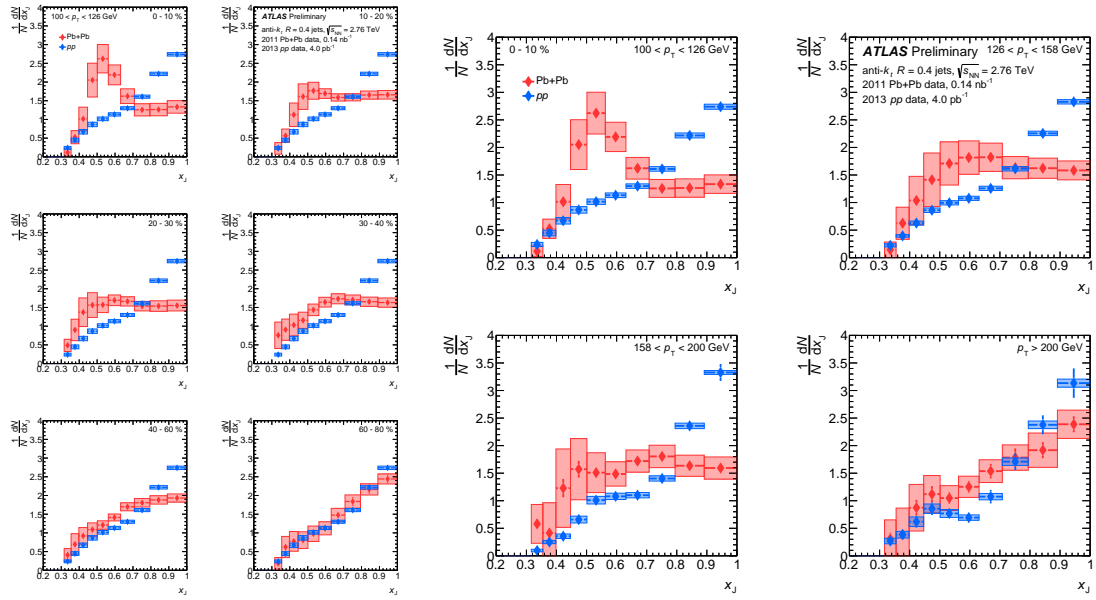


Fig. 3. Per-dijet pair  $x_J$  distributions in  $\text{Pb}+\text{Pb}$  (red) and  $pp$  collisions (blue), fully corrected to the particle level, from Ref. [5]. The vertical lines and boxes show the statistical and systematic uncertainties, respectively. a)  $p_{\text{T},1} > 100$  GeV dijet events, each panel showing a different  $\text{Pb}+\text{Pb}$  centrality selection. b) 0-10%  $\text{Pb}+\text{Pb}$  events, each panel showing a different selection on  $p_{\text{T},1}$ .

indicates that for systematically higher selections on the leading jet  $p_{\text{T}}$ , while both jets may be individually quenched, the most likely dijet configurations are nevertheless balanced. The observed  $p_{\text{T},1}$  dependence may suggest, for example, a decrease in the fractional energy loss with increasing  $p_{\text{T}}$ .

## 5. Conclusion

This work presents an updated measurement of the dijet transverse momentum balance distributions in  $\text{Pb}+\text{Pb}$  collisions with the ATLAS detector at the LHC. The distributions have been corrected for detector effects to the particle level, and are presented as a function of the event centrality and leading jet  $p_{\text{T}}$ . For dijets with  $p_{\text{T},1} > 100$  GeV in the most central collisions, the typical configurations are strongly asymmetric compared to that in  $pp$  collisions at the same collision energy. However, in peripheral collisions or at higher  $p_{\text{T},1}$  ( $> 200$  GeV), the distributions are qualitatively similar to those in  $pp$  collisions, providing insight into the differential path-length-dependent energy loss in the hot nuclear matter created in these collisions.

## References

- [1] ATLAS Collaboration, Phys. Rev. Lett. 105 (2010) 252303; CMS Collaboration, Eur. Phys. J. C74 (2014) 2951.
- [2] CMS Collaboration, Phys. Rev. C84 (2011) 024906.
- [3] C. E. Coleman-Smith, B. Müller, Phys. Rev. C86 (2012) 054901; Y. He, I. Vitev, B.-W. Zhang, Phys. Lett. B713 (2012) 224–232; C. Young, B. Schenke, S. Jeon, C. Gale, Phys. Rev. C84 (2011) 024907.
- [4] ATLAS Collaboration, ATLAS-CONF-2015-016, <http://cdsweb.cern.ch/record/2008677>.
- [5] ATLAS Collaboration, ATLAS-CONF-2015-052, <http://cdsweb.cern.ch/record/2055673>.
- [6] ATLAS Collaboration, Phys. Rev. Lett. 114 (2015) 072302; ATLAS Collaboration, ATLAS-CONF-2015-021, <http://cdsweb.cern.ch/record/2029371>; ATLAS Collaboration, Phys. Lett. B751 (2015) 376
- [7] ATLAS Collaboration, JINST 3 (2008) S08003.
- [8] ATLAS Collaboration, Phys. Lett. B719 (2013) 220; ATLAS Collaboration, Phys. Lett. B748 (2015) 392.
- [9] S. Agostinelli et al., Nucl. Instrum. Meth. A 506 (2003) 250; ATLAS Collaboration, Eur. Phys. J. C70 (2010) 823.
- [10] T. Sjostrand, S. Mrenna and P. Z. Skands, JHEP 0605 (2006) 026; Comput. Phys. Commun. 178 (2008) 852.
- [11] G. D'Agostini, Nucl. Instrum. Meth. A362 (1995) 487.